Contribution of space charges to the polarization of ferroelectric superlattices and its effect on dielectric properties

M. B. Okatan,[1] I. B. Misirlioglu,[2] and S. P. Alpay[1,3,*]

[1]*Materials Science and Engineering Program, Department of Chemical, Materials, and Biomolecular Engineering, University of Connecticut, Storrs, Connecticut 06269, USA*

[2]*Faculty of Engineering and Natural Sciences, Sabancı University, Tuzla-Orhanlı 34956, Istanbul, Turkey*

[3]*Department of Physics, University of Connecticut, Storrs, Connecticut 06269, USA*

(Received 16 April 2010; revised manuscript received 15 July 2010; published 22 September 2010)

A theoretical model is developed for ferroelectric bilayers and multilayer heterostructures that employs a nonlinear Landau-Devonshire formalism coupled with a detailed analysis of the depolarizing fields arising from the polarization mismatch across interlayer interfaces and the electrical fields of localized space charges at such interfaces. We first present how space charges alter the free-energy curves of ferroelectrics and then proceed with a numerical analysis for heteroepitaxial (001) $PbTiO_3$-$SrTiO_3$ (PTO-STO) bilayers and (001) superlattice structures on (001) STO substrates. The switchable (ferroelectric) and nonswitchable (built-in) polarizations and the dielectric properties of PTO-STO bilayers and superlattices are calculated as a function of the planar space-charge density and the volume fraction of the PTO layer. Similar to the temperature dependence of a monolithic ferroelectric, there exists a critical volume fraction PTO below which the bilayer or the superlattice is in the paraelectric state. This critical volume fraction is strongly dependent on the density of trapped charges at the interlayer interfaces. For charge-free (001) PTO-STO heteroepitaxial bilayer and superlattices, the critical fraction is 0.40 for both constructs but increases to 0.6 and 0.72, for the bilayer and the superlattice, respectively, for a planar space-charge density of 0.05 C/m^2. Furthermore, our results show that close to the vicinity of ferroelectric-paraelectric phase transition, there is a recovery in ferroelectric polarization. The dielectric-response calculations verify that there is sharp ferroelectric phase transformation for charge-free bilayers and superlattices whereas it is progressively smeared out with an increase in the charge density. Furthermore, our analysis shows that the dielectric constant of these multilayers at a given volume fraction of PTO decreases significantly in the presence of space charges.

DOI: 10.1103/PhysRevB.82.094115 PACS number(s): 77.80.bn, 77.55.Px

I. INTRODUCTION

Ferroelectric thin films and nanostructures have gained significant interest in recent years due to their unique properties and potential applications. With advances in the deposition techniques, ferroelectric multilayers and superlattices can now be grown with exceptional compositional and structural control even as ultrathin films that may scale down to a couple of lattice parameters.[1–5] It is not the intention of this study to provide an extensive review of the numerous experimental and theoretical findings on several different ferroelectric multilayers in the past decade. However, on the experimental side some noteworthy examples include ultrathin superlattice heterostructures composed of $BaTiO_3$, $SrTiO_3$, and $CaTiO_3$ layers that display a clear polarization enhancement when compared to monolayer $BaTiO_3$ films deposited under same conditions[6] and a large dielectric permittivity that depends on the stacking sequence of the superlattice.[7] Theoretically, the behavior of ferroelectric multilayers has been described through first-principles simulations,[8–10] electrostatic considerations,[11–13] and mechanistic approaches taking into account domain phenomena.[14] Phase field simulations show that it is possible to form new domain patterns in simple ferroelectric-dielectric bilayers and in graded ferroelectric heterostructures.[15,16]

Keeping in mind the propensity of interlayer interfaces to serve both as nucleation sites and as hosts for numerous defects owing to the nature of the deposition processes, it is more likely to encounter such structural and electrical perturbations in multilayers and superlattices. We considered localized, i.e., immobile, space charges whose physical origin in fully depleted ferroelectric films can be either oxygen vacancies or deep trapping centers.[17] Therefore, space charges were assumed to be localized at the interlayer interfaces giving rise to planar space charges. It is known from the detailed work of Bratkovsky and Levanyuk that (localized) space charges have prominent effects on phase-transition characteristics in monolithic ferroelectrics[18] that may lead to the suppression of the ferroelectric phase transformation temperature by as much as 100 °C. Furthermore, Zubko *et al.*[19,20] investigated the hysteresis response of fully and partially depleted monolithic ferroelectrics in the case of homogeneous space-charge distributions. Their results demonstrate that hysteresis loops progressively shrink with increasing space-charge densities. Possible leakage mechanisms such as space-charge limited conduction, Schottky thermionic emission under full and partial depletion and Poole-Frenkel conduction were investigated as well.[20] Our own results[21–23] show that if there are charged defects to compensate for the polarization mismatch and relax the depolarization fields, ferroelectric multilayers may behave independently from each other and exhibit a dielectric response that can be described as the sum of their corresponding intrinsic uncoupled dielectric properties. For perfectly insulating heterostructures with no localized charges, the depolarization field is minimized by lowering the polarization difference between lay-

ers, yielding a ferroelectric multilayer that behaves as if it were a single ferroelectric material.[21] In addition, our findings show that the polarization hysteresis response of homogeneous stress-free ferroelectrics with asymmetrically distributed space charges result in a displacement of the hysteresis loop along the applied electric field axis. In compositionally graded ferroelectric multilayers, the hysteresis is characterized by offsets along both the polarization and electric field axes with magnitudes of displacement that are significantly larger than those for monolithic ferroelectrics.[23] We note that these theoretical studies mentioned above on the effect of space charges all rely on the continuity of the normal component of the electric displacement field at interface boundaries which results in polarization variations and hence a commensurate depolarizing field. It was pointed out as early as 1986 that contribution of the background dielectric constant (ε_b) could be crucial in explaining the dielectric response of uniaxial ferroelectrics.[24] The importance of this, especially in such cases where a depolarizing field is involved, has been recently emphasized by Tagantsev and Bratkovsky and Levanyuk wherein it is stated that for a proper description of electrostatic boundary conditions ε_b has to be taken into account.[17,25,26]

Therefore, considering potential applications of multilayer ferroelectrics in tunable devices for telecommunications, as elements of memory devices (dynamic and nonvolatile random access memories), and in infrared sensors, it is crucial to understand how space charges that invariably exist in these heterostructures would affect their polarization response and dielectric properties. This is the main objective of this study wherein we provide a comprehensive analysis of ferroelectric multilayers with localized space charges at the interlayer interfaces building upon our previous analysis[23] and taking into account the background dielectric constant. Our approach employs a nonlinear Landau-Devonshire formalism coupled with a detailed analysis of the depolarizing fields arising from the polarization mismatch across interlayer interfaces and the electrical fields of the space charges. We present numerical results for heteroepitaxial (001) $PbTiO_3$-$SrTiO_3$ (PTO-STO) bilayers and (001) superlattice structures on (001) STO substrates. The switchable and nonswitchable polarizations and the dielectric properties of PTO-STO bilayers and superlattices are calculated as a function of the linear space-charge density and the volume fraction of the PTO layer. Our results show that the dielectric constant of these multilayers at a given volume fraction of PTO is greatly reduced in the presence of space charges.

II. THEORY

In our analysis, we consider a heteroepitaxial ferroelectric heterostructure made up of n single-domain layers sandwiched between electrodes (Fig. 1). In order to represent a general case of space-charge distribution, it is assumed that each interlayer interface may accommodate different amounts of localized space charges. The total electric field in such a heterostructure is governed by the electrostatic boundary conditions which are given by: (i) the continuity of the normal component of the electric displacement field at each

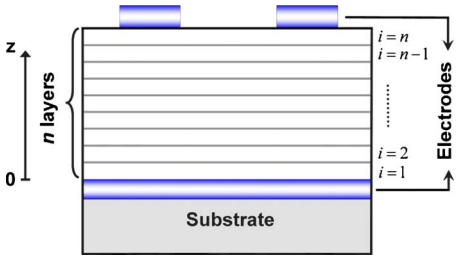

FIG. 1. (Color online) The schematic representation of the ferroelectric heterostructure for the theoretical analysis.

interlayer interface and (ii) the total electrical potential difference, V, between the electrodes. According to the orientation of z axis and the layer designations depicted in Fig. 1, conditions (i) and (ii) can be written, respectively, as

$$(P_{i+1} - P_i) + \varepsilon_0(\varepsilon_{b,i+1}E_{i+1} - \varepsilon_{b,i}E_i) = \sigma_{i,i+1}$$

$$i = 1,2,\ldots,(n-1), \tag{1}$$

$$\sum_{i=1}^{n} \ell_i E_i = V = LE^{ext}. \tag{2}$$

Here, P_i, E_i, $\varepsilon_{b,i}$, ℓ_i, and ε_0 are the polarization, the total electric field in layer i, the background dielectric constant, the thickness of layer i, and the permittivity of free space, respectively. $\sigma_{i,i+1}$ is the planar space-charge density located at the interlayer interface between ith and $(i+1)$th layers, and E^{ext} is the externally applied electric field between the electrodes, resulting from the externally induced electrical potential difference V across the thickness of the heterostructure $L=\Sigma_{k=1}^{n}\ell_k$.

Solution of the system of equations given by Eqs. (1) and (2) for E_i $(i=1,2,\ldots,n)$ yields

$$E_i = E_i^{ext} + E_i^D + E_i^{sc}, \tag{3}$$

where

$$E_i^{ext} = \frac{E^{ext}}{\varepsilon_{b,i}\varphi}, \tag{4}$$

$$E_i^D = -\frac{1}{\varepsilon_0\varepsilon_{b,i}}\left(P_i - \frac{1}{\varphi}\sum_{j=1}^{n}\frac{\alpha_j}{\varepsilon_{b,j}}P_j\right), \tag{5}$$

$$E_i^{sc} = -\frac{1}{\varepsilon_0\varepsilon_{b,i}}\left[\sum_{i}^{n}\sigma_{i,i+1} - \frac{1}{\varphi}\sum_{j=1}^{n}\left(\sum_{k=1}^{j}\frac{\alpha_k}{\varepsilon_{b,k}}\right)\sigma_{j,j+1}\right], \tag{6}$$

$$\varphi = \sum_{j=1}^{n}\frac{\alpha_j}{\varepsilon_{b,j}}. \tag{7}$$

Here $\alpha_i=\ell_i/L$ is the volume fraction of layer i. E_i^{ext} is the strength of the externally applied electric field in layer i. Taking into account the background dielectric constant of each layer reflects the heterogeneous nature of the medium, i.e., the ferroelectric heterostructure, placed between the electrodes. Depending on the value of the product $\varepsilon_{b,i}\varphi$

which can be greater or smaller than unity, the externally applied electric field E^{ext} seen by layer i is either attenuated or amplified. Such a variation in E_i^{ext} is absent for a homogeneous medium such as a *monolithic* ferroelectric since $\varepsilon_{b,i}\varphi=1$. E_i^D is the depolarizing electric field in layer i arising as a consequence of inhomogeneous polarization distribution across the heterostructure, although polarization P_i in each layer is homogeneous. E_i^{sc} is the electric field generated in layer i due to space charges $\sigma_{j,j+1}$ located at each interlayer interfaces. We note that the value of $\sigma_{n,n+1}$ has no bearing on the findings and it can be set equal to zero; but it is introduced to allow us to express Eq. (6) in a more compact form. Furthermore, both E_i^D and E_i^{sc} do not induce a potential difference between the electrodes, i.e., $\Sigma_{i=1}^n \alpha_i E_i^D=0$ and $\Sigma_{i=1}^n \alpha_i E_i^{sc}=0$ but $\Sigma_{i=1}^n \alpha_i E_i^{ext}=E^{ext}$. Thus, in the absence of the externally applied electric field the monolithic/heterostructure capacitor is under short-circuit conditions. In the case of ultrathin films in which the spatial distribution of polarization is mainly affected and determined due to electromechanical conditions at the surfaces/interfaces, the electrostatic boundary conditions employed in our model (infinite extrapolation length) needs to be modified to take into account for finite values of extrapolation length. We have refrained to do so since we consider superlattices in which each individual layer is thick enough to avoid surface related effects. Furthermore, it is somewhat not clear which boundary conditions should be employed in such an analysis.[19] We note that our model that is described through Eqs. (1)–(7) is scale independent, i.e., the thermodynamic potential changes with respect to *relative thicknesses* and not with the *actual thicknesses* of layers which is a direct consequence of the electrostatic boundary conditions considered. For ultrathin layers that are of thicknesses on the order of the correlation length of ferroelectricity (1–10 nm),[27] polarization gradient terms have to be included in the free-energy functional which will naturally give rise to equations of state that are dependent on the actual thicknesses of layers.

Therefore, the total free-energy density of an n-layered ferroelectric heterostructure is given as

$$F_\Sigma = \sum_{i=1}^{n} \alpha_i(\Phi_i - E_i^{ext}P_i) - \frac{1}{2}\sum_{i=1}^{n} \alpha_i E_i^D P_i - \sum_{i=1}^{n} \alpha_i E_i^{sc} P_i, \quad (8)$$

where

$$\Phi_i = \Phi_{0,i} + \frac{1}{2}a_i' P_i^2 + \frac{1}{4}b_i' P_i^4 + \frac{1}{6}c_i P_i^6 + \frac{x_i^2}{s_{11,i}+s_{12,i}} \quad (9)$$

is the Landau expansion of the free energy of the ith layer with the polarization P_i as the order parameter. Here, we employ renormalized coefficients a_i' and b_i' to take into account the epitaxial strain and the two-dimensional clamping of the substrate,

$$a_i' = a_i - x_i \frac{4Q_{12,i}}{s_{11,i}+s_{12,i}}, \quad (10)$$

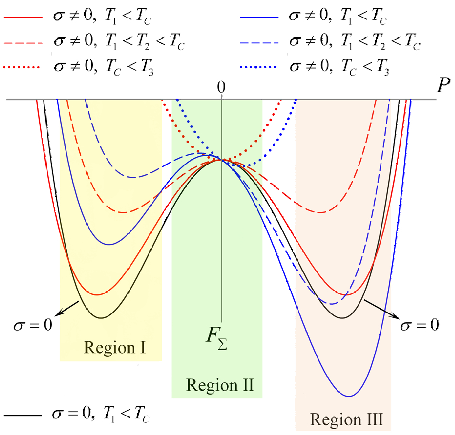

FIG. 2. (Color online) Schematic representation of F_Σ-P curves of a *monolithic* ferroelectric at different temperatures and $E^{ext}=0$. The curves that are symmetric (asymmetric) with respect to the vertical F_Σ axis show the variation in F_Σ of a *monolithic* ferroelectric in which *inhomogeneously* distributed space charges (do not) possess mirror symmetry with respect to the mid-section of the film such that $P \equiv \langle P \rangle$ and $\langle P_{ns} \rangle = 0$ *always* ($P \equiv \langle P \rangle$ and $\langle P_{ns} \rangle \neq 0$ *always*). The condition for which $\sigma=0$ is also shown as a reference.

$$b_i' = b_i + \frac{4Q_{12,i}^2}{s_{11,i}+s_{12,i}}, \quad (11)$$

where a_i, b_i, and c_i are the unconstrained bulk dielectric stiffness coefficients of layer i.[28] The temperature dependence of the a_i is given by the Curie-Weiss law such that $a_i=(T-T_{C,i})/\varepsilon_0 C_i$, where $T_{C,i}$ and C_i are the Curie temperature and constant of layer i, respectively. In Eqs. (9) and (10), $x_i=(\xi_s-\xi_i)/\xi_s$ is the pseudocubic polarization-free misfit (epitaxial) strain in layer i and ξ_s and ξ_i are the lattice constants of the substrate and layer i in its cubic paraelectric state, respectively. $Q_{mn,i}$ and $s_{mn,i}$ are the electrostrictive coefficients and elastic compliances of layer i, respectively. $\Phi_{0,i}$ in Eq. (9) is the free-energy density of the polarization-free high-temperature paraelectric phase. The equilibrium polarizations P_i are determined as solutions to the system of equations of state given as $\partial F_\Sigma/\partial P_i=0$ for $i=1,2,\ldots,n$, where

$$\frac{\partial F_\Sigma}{\partial P_i} = \alpha_i(a_i' P_i + b_i' P_i^3 + c_i P_i^5 - E_i^{ext} - E_i^D - E_i^{sc}). \quad (12)$$

Depending on the nature of the medium being homogeneous or heterogeneous, and the way space charges are distributed in that medium between the electrodes, solutions satisfying Eq. (12) will possess quite different values and temperature-dependent behavior. Referring to Fig. 2. that schematically shows the variation in total free energy with respect to polarization in the absence of E^{ext}, we will briefly explain these possible scenarios. The extrema corresponding to (local) minimum, maximum and (global) minimum satisfying Eq. (12) are shown, respectively, in Regions I, II, and III for various temperatures T_1, $T_2<T_C$, and $T_3>T_C$. A monolithic ferroelectric with no space charges ($\sigma=0$) will exhibit two energetically equivalent stable polarization states $-P$ (Region I) and $+P$ (Region III) along with an unstable polarization state at $P=0$ (Region II) below its ferroelectric-

TABLE I. Thermodynamic parameters of bulk PTO and bulk STO used in this study; $(s_{11}+s_{12})^{-1}=c_{11}+c_{12}-2c_{12}^2/c_{11}$.

	PTO	STO
T_C (°C)	479	−253
C (°C)	1.5×10^5	0.8×10^5
b (N m^6/C^4)	-2.92×10^8	8.4×10^9
c (N m^{10}/C^6)	1.56×10^9	
c_{11} (N/m^2)	1.75×10^{11}	3.181×10^{11}
c_{12} (N/m^2)	7.94×10^{10}	1.025×10^{11}
Q_{12} (m^4/C^2)	−0.026	−0.013
$\tilde{n}$ (@ 633 nm)	2.67	2.39
ξ (Å) @ 25 °C	3.947	3.905

paraelectric phase-transition temperature T_C. This unstable polarization state is referred to as the nonswitchable or the built-in polarization, P_{ns}.[18] In the case of a monolithic ferroelectric in which space charges are distributed *homogeneously* where such a distribution can be approximately represented by dividing the ferroelectric into equally thick layers and placing space charges of same planar density at each interlayer interface, the unstable polarization state in layer i ($P_{ns,i}$) attains a finite value if $E_i^{sc}\neq0$ and the sign of $P_{ns,i}$ depends on the direction of E_i^{sc}. In this case, $P_{ns,i}$ will possess an extremely negligible temperature dependence and thus remains almost *insensitive* to the phase transition.[18] In addition to that no smearing will be observed around T_C.[18] In general, for a monolithic ferroelectric in which *inhomogeneously* distributed space charges possess a symmetric distribution with respect to the middle of the film, $P_{ns,i}$ stays almost independent of temperature and smearing of the phase transition does not take place. Furthermore, in a monolithic ferroelectric where the charges are asymmetrically arranged, the nonswitchable (built-in) polarization $P_{ns,i}$ exhibits an appreciable temperature dependency in the vicinity of T_C and the phase transition is smeared as if an externally applied electric field exists. In the paraelectric phase ($T_3>T_C$), $P_{ns,i}$ is the only solution. The switchable (ferroelectric) polarization of layer i is given by the difference between total polarization and nonswitchable polarization, $P_{sw,i}=P_i-P_{ns,i}$.

The average polarization $\langle P\rangle$ of the heterostructure can be calculated from the equilibrium polarizations as

$$\langle P\rangle=\sum_{i=1}^{n}\alpha_i P_i \tag{13}$$

and the dielectric constant ε of the heterostructure can be determined via the definition of the dielectric constant as

$$\varepsilon=\frac{1}{\varepsilon_0}\frac{\partial D_i}{\partial E^{ext}}. \tag{14}$$

In Eq. (14), one can use the electric displacement field $D_i=\varepsilon_0\varepsilon_{b,i}E_i+P_i$ of any one of the layers as the variation in D_i with respect to E^{ext} is independent of $\sigma_{i,i+1}$ since $D_{i+1}-D_i=\sigma_{i,i+1}$ which results in $\partial D_{i+1}/\partial E^{ext}=\partial D_i/\partial E^{ext}$.

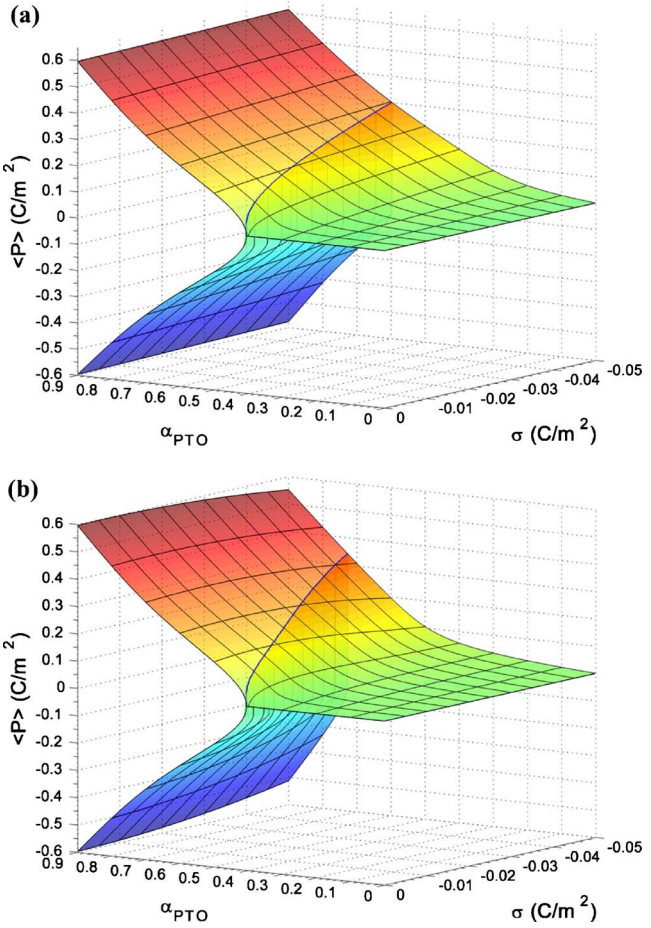

FIG. 3. (Color online) The variation in the average polarization $\langle P\rangle$ with volume fraction of PTO (α_{PTO}) and planar space-charge density (σ) for (a) bilayer ($n=2$) and (b) superlattice ($n=10$) PTO-STO structures at room temperature in the absence of E^{ext}. The solid lines transversing each graph along the σ axis marks the boundary between paraelectric and ferroelectric phases.

III. RESULTS AND DISCUSSION

For a quantitative analysis, we considered a bilayer ($n=2$) and a superlattice ($n=10$) of (001) PTO and (001) STO layers on (001) STO substrates where the superlattice structure corresponds to five adjacent PTO-STO bilayers. Moreover, each interlayer interface was assumed to accommodate the same amount of localized space charges of planar charge density $\sigma_{i,i+1}=\sigma$ for all i. This leads to a simplification of Eq. (6) to

$$E_i^{sc}=-\frac{\sigma}{\varepsilon_0\varepsilon_{b,i}}\left[(n-i)-\frac{1}{\varphi}\sum_{j=1}^{n}\frac{\alpha_j}{\varepsilon_{b,j}}(n-j)\right]. \tag{15}$$

Material constants of PTO and STO employed in this study are given in Table I.[14,28] The background dielectric constant was taken as $\varepsilon_b=\tilde{n}^2$, where $\tilde{n}$ is the optical frequency refractive index.[29] Room-temperature pseudocubic/cubic lattice parameters of PTO and STO was determined via best fitting to the cubic phase lattice parameters from Refs. 30 and 31, respectively.

Dependence of the average polarization $\langle P \rangle$ on the volume fraction of PTO α_{PTO} and planar space-charge density σ are shown in Figs. 3(a) and 3(b), respectively, for PTO-STO bilayer and superlattice structures at room temperature. The solid line transversing the three-dimensional graphs along the σ axis marks the boundary between paraelectric and ferroelectric phases. It represents the combinations of bilayer/superlattice structures and space charges for which the phase-transition temperature corresponds to 25 °C (room temperature). Referring to our own results for multilayered ferroelectrics,[23] it can be easily noticed that there exist similar trends between $\langle P \rangle$-α_{PTO}-σ and $\langle P \rangle$-T-σ plots where a decrease in α_{PTO} is analogous to an increase in T. As such, $\langle P \rangle$-α_{PTO}-σ plots at a given temperature as shown in Fig. 3 can be qualitatively thought of as $\langle P \rangle$-T-σ plots at a given α_{PTO} and vice versa. As σ is increased, paraelectric to ferroelectric phase transition occurs at higher α_{PTO} values. This shift of phase-transition boundary is expected to take place since it is known that incorporation of space charges into monolithic and heterogeneous ferroelectrics suppresses phase-transition temperature.[18,23] Thus, to maintain ferroelectricity in the heterostructure, the volume fraction of the ferroelectrically "harder" component (α_{PTO}) has to be increased in order to compensate the decline in phase-transition temperature due to space charges. Compared to the bilayer, the suppression of phase-transition temperature is more severe in the superlattice structure since it accommodates higher density of space charges per volume of the heterostructure. Hence, at a fixed σ, paraelectric to ferroelectric phase transition takes place at higher α_{PTO} values in the superlattice with respect to the bilayer. Furthermore, the phase transition is smeared and the stability balance between positive and negative polarization states is broken to favor equilibrium solutions of polarizations for which the average is positive.

In the paraelectric phase, $\langle P \rangle$ corresponds to the average nonswitchable polarization $\langle P_{ns} \rangle$ plotted in Fig. 4. On the other hand, in the ferroelectric phase $\langle P_{ns} \rangle$, which attains negative values in this study, represents the unstable solution accompanying $\langle P \rangle$. It is clearly seen that $\langle P_{ns} \rangle$ is highly sensitive to the phase transition such that it exhibits an appreciable temperature-dependent behavior along the paraelectric-ferroelectric phase boundary.

Figure 5 shows the average switchable polarization $\langle P_{sw} \rangle$ of PTO-STO heterostructures at room temperature as a function of the ratio of the volume fractions of the constituting phases $\alpha_{PTO}/\alpha_{STO}$ for various values of σ. Both in bilayer and superlattice structures $\langle P_{sw} \rangle$ displays a similar behavior. In heterostructures which are free from space charges, $\langle P_{sw} \rangle$ vanishes smoothly with decreasing α_{PTO}. However, if space charges are present in the heterostructures, a slight recovery in $\langle P_{sw} \rangle$ is seen with decreasing α_{PTO} in the vicinity of the ferroelectric to paraelectric phase transition. This recovery in $\langle P_{sw} \rangle$ occurs due to the temperature-dependent behavior of $\langle P_{ns} \rangle$. It is clearly noticeable that as space charges are introduced into the heterostructures, the paraelectric-ferroelectric phase transition is shifted to higher values of α_{PTO} and the magnitude of this shift is more pronounced in the superlattice structure considered. We note that these results differ from the previous analysis of Misirlioglu *et al.*[32] wherein the planar space-charge density was presumed to be equal to the built-in polarization difference. In that study, polarization was considered to consist of two components, a switchable component and a built-in component with the latter being temperature insensitive. Dawber *et al.*[33,34] have reported that there is a recovery of switchable polarization for $\alpha_{PTO} < 0.4$ in PTO-STO superlattices. According to this study, the observed recovery in switchable polarization in PTO-STO superlattices may not necessarily be due to space charges[32] but due to other microscopic mechanisms. Our theoretical findings indicate that if localized space charges were indeed responsible for such a recovery in these ferroelectric heterostructures this may be possible for $\alpha_{PTO} > 0.4$.

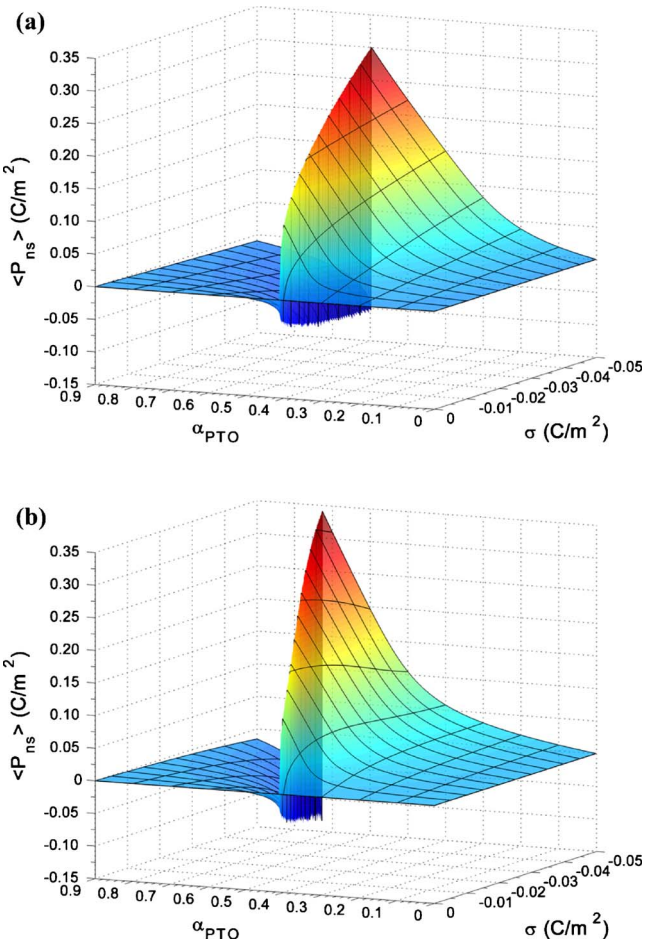

FIG. 4. (Color online) The variation in the average nonswitchable polarization $\langle P_{ns} \rangle$ with volume fraction of PTO (α_{PTO}) and planar space-charge density (σ) for (a) bilayer ($n=2$) and (b) superlattice ($n=10$) PTO-STO structures at room temperature in the absence of E^{ext}.

The dielectric constants ε of heterostructures are shown as a function of α_{PTO} and σ in Fig. 6. In the absence of space charges, ε exhibits a diverging behavior at the paraelectric-ferroelectric phase transition $\alpha_{PTO} \approx 0.4$. However, a gradual decrease in peak value of ε along with a widening in the peak is seen upon increasing σ. This diffusive transition response in ε is due to smearing of the phase transition. The maximum in ε occurs in the paraelectric phase as in the case of a ferroelectric material subjected to an externally applied electric field.[18,27]

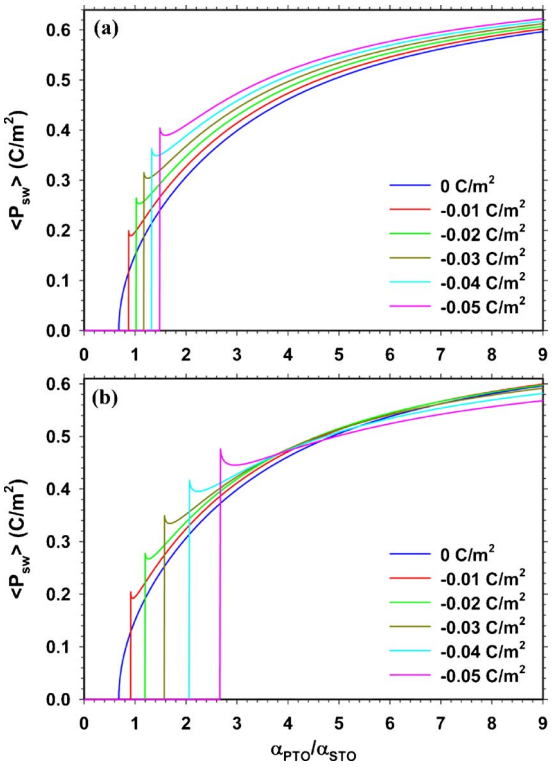

FIG. 5. (Color online) The variation in the average switchable polarization $\langle P_{ns} \rangle$ in (a) bilayer ($n=2$) and (b) superlattice ($n=10$) PTO-STO structures as a function of the ratio of the volume fraction of the layers ($\alpha_{PTO}/\alpha_{STO}$) at various values of σ at room temperature in the absence of E^{ext}.

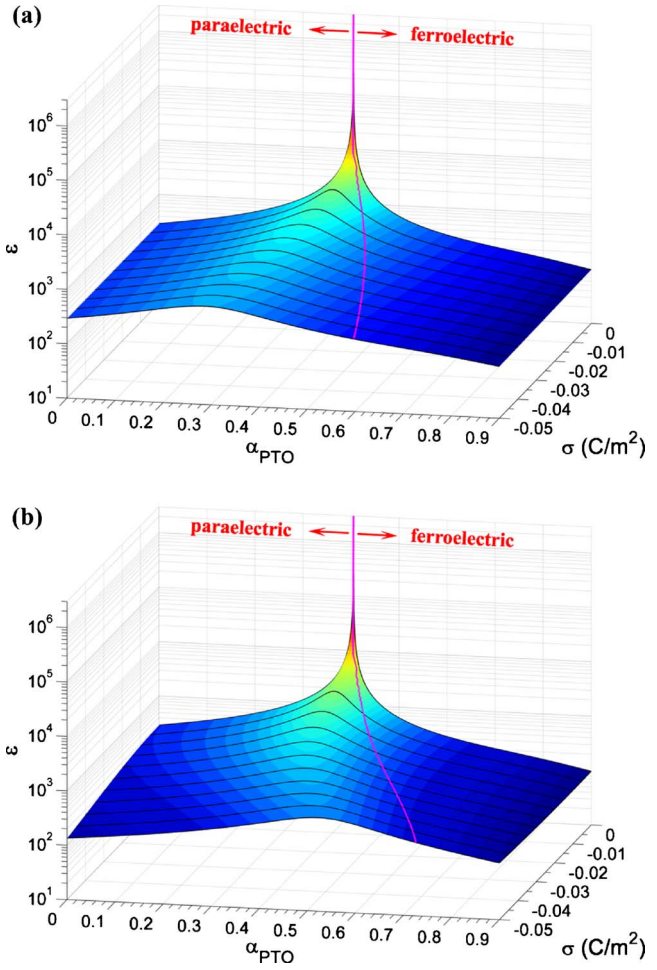

FIG. 6. (Color online) The variation in the dielectric constant ε as a function of the volume fraction of PTO (α_{PTO}) and the planar space-charge density (σ) for (a) bilayer ($n=2$) and (b) superlattice ($n=10$) PTO-STO structures at room temperature in the absence of E^{ext}. The solid lines transversing each graph along the σ axis marks the boundary between paraelectric and ferroelectric phases.

IV. CONCLUSIONS

In summary, we have presented herein a theoretical analysis that describes the polarization behavior and dielectric properties of ferroelectric heterostructures with localized space charges at the interlayer interfaces. Although the theory has been specifically applied to ferroelectric superlattices, this study contains all the theoretical tools that can be used, with appropriate adjustments, to describe any monolithic ferroelectric, compositionally graded ferroelectrics, and multilayer ferroelectrics and their dielectric properties as a function of space-charge concentration. The findings for heteroepitaxial (001) PTO-STO bilayers and (001) superlattice structures on (001) STO substrates show that if the heterostructure is charge free, the critical PTO fraction at which the ferroelectric phase transformation occurs is 0.40 but this changes to 0.6 and 0.72 for the bilayer and the superlattice, respectively, for a planar space-charge density of 0.05 C/m^2; in the vicinity of this critical α_{PTO}, the built-in polarization due to space charges shows appreciable variation in both types of heterostructures; these variations result in a recovery in the switchable polarization near critical α_{PTO}; the sharp ferroelectric phase transformation for charge-free bilayers and superlattices is smeared out with an increase in the charge density; and the dielectric constants of charge-free bilayers and superlattices are significantly reduced in the presence of space charges at a given α_{PTO}.

While the theoretical model employed in this study corresponds to a simplified condition that assumes a constant σ at the interlayer interfaces, it nonetheless provides a clear understanding of the effect of space charges in multilayer ferroelectrics. The findings indicate the need for synthesis/processing conditions that would produce minimum amount of space charges in the ferroelectric superlattices for these heterostructures to be considered in device applications.

ACKNOWLEDGMENTS

I.B.M. acknowledges the hardware and software support of Sabanci University. The work at the University of Connecticut was funded by the U.S. Army Research Office through Grants No. W911NF-05-1-0528 and No. W911NF-08-C-0124.

*p.alpay@ims.uconn.edu

[1] J. M. Gregg, J. Phys.: Condens. Matter **15**, V11 (2003).
[2] C. H. Ahn, K. M. Rabe, and J. M. Triscone, Science **303**, 488 (2004).
[3] D. D. Fong, G. B. Stephenson, S. K. Streiffer, J. A. Eastman, O. Auciello, P. H. Fuoss, and C. Thompson, Science **304**, 1650 (2004).
[4] D. G. Schlom, L.-Q. Chen, C.-B. Eom, K. M. Rabe, S. K. Streiffer, and J.-M. Triscone, Annu. Rev. Mater. Res. **37**, 589 (2007).
[5] I. Vrejoiu, M. Alexe, D. Hesse, and U. Gösele, Adv. Funct. Mater. **18**, 3892 (2008).
[6] H. N. Lee, H. M. Christen, M. F. Chisholm, C. M. Rouleau, and D. H. Lowndes, Nature (London) **433**, 395 (2005).
[7] M. P. Warusawithana, E. V. Colla, J. N. Eckstein, and M. B. Weissman, Phys. Rev. Lett. **90**, 036802 (2003).
[8] J. B. Neaton and K. M. Rabe, Appl. Phys. Lett. **82**, 1586 (2003).
[9] S. M. Nakhmanson, K. M. Rabe, and V. David, Appl. Phys. Lett. **87**, 102906 (2005).
[10] S. M. Nakhmanson, K. M. Rabe, and D. Vanderbilt, Phys. Rev. B **73**, 060101 (2006).
[11] L. Pintilie, I. Boerasu, and M. J. M. Gomes, J. Appl. Phys. **93**, 9961 (2003).
[12] A. L. Roytburd, S. Zhong, and S. P. Alpay, Appl. Phys. Lett. **87**, 092902 (2005).
[13] A. N. Morozovska and E. A. Eliseev, Phys. Status Solidi B **242**, 947 (2005).
[14] M. B. Okatan, A. L. Roytburd, J. V. Mantese, and S. P. Alpay, J. Appl. Phys. **105**, 114106 (2009).
[15] Y. L. Li, S. Y. Hu, D. Tenne, A. Soukiassian, D. G. Schlom, X. X. Xi, K. J. Choi, C. B. Eom, A. Saxena, T. Lookman, Q. X. Jia, and L. Q. Chen, Appl. Phys. Lett. **91**, 112914 (2007).
[16] A. Artemev, B. Geddes, J. Slutsker, and A. Roytburd, J. Appl. Phys. **103**, 074104 (2008).
[17] A. K. Tagantsev and G. Gerra, J. Appl. Phys. **100**, 051607 (2006).
[18] A. M. Bratkovsky and A. P. Levanyuk, Phys. Rev. B **61**, 15042 (2000).
[19] P. Zubko, D. J. Jung, and J. F. Scott, J. Appl. Phys. **100**, 114112 (2006).
[20] P. Zubko, D. J. Jung, and J. F. Scott, J. Appl. Phys. **100**, 114113 (2006).
[21] M. B. Okatan, J. V. Mantese, and S. P. Alpay, Phys. Rev. B **79**, 174113 (2009).
[22] M. B. Okatan and S. P. Alpay, Appl. Phys. Lett. **95**, 092902 (2009).
[23] M. B. Okatan, J. V. Mantese, and S. P. Alpay, Acta Mater. **58**, 39 (2010).
[24] A. K. Tagantsev, Ferroelectrics **69**, 321 (1986).
[25] A. K. Tagantsev, Ferroelectrics **375**, 19 (2008).
[26] A. M. Bratkovsky and A. P. Levanyuk, J. Comput. Theor. Nanos. **6**, 465 (2009).
[27] B. A. Strukov and A. P. Levanyuk, *Ferroelectric Phenomena in Crystals: Physical Foundations* (Springer-Verlag, Berlin, 1998).
[28] N. A. Pertsev, A. G. Zembilgotov, and A. K. Tagantsev, Phys. Rev. Lett. **80**, 1988 (1998).
[29] M. Bass, *Handbook of Optics: Devices, Measurements, and Properties*, 2nd ed. (McGraw-Hill Professional, New York, 1994), Vol. 2.
[30] J. Chen, X. Xing, R. Yu, and G. Liu, J. Am. Ceram. Soc. **88**, 1356 (2005).
[31] M. D. Biegalski, J. H. Haeni, S. Trolier-McKinstry, D. G. Schlom, C. D. Brandle, and A. J. Ven Graitis, J. Mater. Res. **20**, 952 (2005).
[32] I. B. Misirlioglu, M. Alexe, L. Pintilie, and D. Hesse, Appl. Phys. Lett. **91**, 022911 (2007).
[33] M. Dawber, N. Stucki, C. Lichtensteiger, S. Gariglio, P. Ghosez, and J. M. Triscone, Adv. Mater. **19**, 4153 (2007).
[34] M. Dawber, C. Lichtensteiger, M. Cantoni, M. Veithen, P. Ghosez, K. Johnston, K. M. Rabe, and J. M. Triscone, Phys. Rev. Lett. **95**, 177601 (2005).